Alterations in Flight Muscle Ultrastructure and Function in *Drosophila* Tropomyosin Mutants

Andrew J. Kreuz,* Amanda Simcox,* and David Maughan‡

*Department of Molecular Genetics, The Ohio State University, Columbus, Ohio 43210; and ‡Department of Molecular Physiology and Biophysics, University of Vermont, Burlington, Vermont 05405

Abstract. *Drosophila* indirect flight muscle (IFM) contains two different types of tropomyosin: a standard 284–amino acid muscle tropomyosin, Ifm-TmI, encoded by the *TmI* gene, and two >400 amino acid tropomyosins, TnH-33 and TnH-34, encoded by *TmII*. The two IFM-specific TnH isoforms are unique tropomyosins with a COOH-terminal extension of ~200 residues which is hydrophobic and rich in prolines. Previous analysis of a hypomorphic *TmI* mutant, *Ifm(3)3*, demonstrated that Ifm-TmI is necessary for proper myofibrillar assembly, but no null *TmI* mutant or *TmII* mutant which affects the TnH isoforms have been reported. In the current report, we show that four flightless mutants (Warmke et al., 1989) are alleles of *TmI*, and characterize a deficiency which deletes both *TmI* and *TmII*. We find that haploidy of *TmI* causes myofibrillar disruptions and flightless behavior, but that haploidy of *TmII* causes neither. Single fiber mechanics demonstrates that power output is much lower in the *TmI* haploid line (32% of wild-type) than in the *TmII* haploid line (73% of wild-type). In myofibers nearly depleted of Ifm-TmI, net power output is virtually abolished (<1% of wild-type) despite the presence of an organized fibrillar core (~20% of wild-type). The results suggest Ifm-TmI (the standard tropomyosin) plays a key role in fiber structure, power production, and flight, with reduced Ifm-TmI expression producing corresponding changes of IFM structure and function. In contrast, reduced expression of the TnH isoforms has an unexpectedly mild effect on IFM structure and function.

TROPOMYOSIN is an α-helical protein which is associated with actin filaments and has a regulatory and structural role in muscle and nonmuscle cells. In striated muscle, tropomyosin (Tm)[1] acts with troponin (Tn) to regulate actomyosin interactions in response to changes in Ca^{2+} concentration (reviewed in El-Saleh et al., 1986; Chalovich, 1993). At low Ca^{2+} concentrations ($<10^{-7}$ M), the Tm-Tn complex prevents the formation of strong, force-generating actomyosin cross-bridges, suppressing the actin-activated Mg^{2+}-ATPase activity of myosin. This suppression is relieved when the Ca^{2+} concentration rises to $\sim10^{-5}$ M.

Models have been proposed to explain the function of tropomyosin. In the steric blocking model (Haselgrove and Huxley, 1973; reviewed in Adelstein and Eisenberg, 1980; El-Saleh et al., 1986; Chalovich, 1993; Squire, 1994) it is proposed that tropomyosin occupies a position on actin that physically blocks myosin crossbridges from binding actin in relaxed muscle (low Ca^{2+}). This inhibition is relieved when troponin, responding to a rise in Ca^{2+}, shifts tropomyosin from a blocking to a nonblocking position on actin. The steric blocking model of muscle regulation is based on evidence from x-ray diffraction patterns and, most recently, three-dimensional reconstruction of thin filament micrographs (Lehman et al., 1994; Reedy et al., 1994*b*). A second model of thin filament regulation, the allosteric or cooperative model, is based primarily on biochemical and fiber studies and expands the role of tropomyosin as a simple blocking protein to that of a more active participant in actomyosin interactions (reviewed in Chalovich, 1993; Lehrer, 1994). In this model, tropomyosin's role is not only to shift and remove a physical block which prevents actomyosin binding but also to facilitate the transition of actin from an "inactive" or "off" (nonmyosin binding) to an "active" or "on" (myosin-binding) state. Despite work directed towards clarifying these models, the precise role of tropomyosin in regulating muscle contraction is still not clear.

A unique tropomyosin, TnH ("heavy" troponin; Bullard et al., 1988), is expressed with standard tropomyosin in the stretch activated indirect flight muscle (IFM) of certain insects (Karlik and Fyrberg, 1986; Bullard et al., 1988;

Address all correspondence to Dr. A.J. Kreuz, Dept. Biological Chemistry, Johns Hopkins School of Medicine, Baltimore, MD. 21205. Ph.: 410-955-6281.

Address reprint requests to A.J. Kreuz or D. Maughan.

1. *Abbreviations used in this paper*: EMS, ethylmethane sulfonate; IFM, indirect flight muscle; Tm, tropomyosin; Tn, troponin.

Hanke and Storti, 1988; Peckham et al., 1992). In *Drosophila*, TnH consists of an NH_2-terminal domain which is homologous to standard muscle tropomyosins joined to a COOH-terminal domain which is hydrophobic and rich in proline residues (Karlik and Fyrberg, 1986; Hanke and Storti, 1988). Although the function of TnH is not known, recent evidence suggests the COOH-terminal domain may form, or be a part of, an extended link between the thin and thick filaments (Bullard et al., 1988; Reedy et al., 1994*a*; Tohtong et al., 1995). Reedy et al. (1994*a*) have shown an epitope on the COOH-terminal hydrophobic portion of TnH is close to the rear cross-bridge of the rigor double chevron in *Lethocerus* IFM, suggesting an intimate TnH–myosin interaction.

Since *Drosophila* asynchronous IFM is activated submaximally by the release of intracellular calcium via intermittent nervous stimulation, a protein link such as TnH connecting thin and thick filaments may be one mechanism by which the muscle is further activated (see below). In isolated, Ca^{2+}-activated IFM, the response to rapid stretch consists of a synchronous tension increase, a rapid decay of tension, and then a significant rise in tension even at constant length. The delayed second rise in tension (called "stretch activation") underlies the ability of all striated muscles to do oscillatory work. Stretch activation is simply a manifestation of cross-bridge cycling (Steiger, 1977; Thorson and White, 1983; Zhao and Kawai, 1993), but the amplitude of stretch-activated tension depends on the muscle type and is especially prominent in insect flight muscle.

Several models have been proposed to explain the enhanced amplitude of stretch activated tension in insect flight muscle. In one model, stretch increases the number of force-generating cross-bridges by increasing the attachment rate constant and/or decreasing the detachment rate constant (Pringle, 1978; Thorson and White, 1983; reviewed in Granzier and Wang, 1993). Granzier and Wang (1993) and Peckham et al. (1992) point out that this model requires a unique strain or stress sensor, possibly TnH, to couple filament strain or stress to elements affecting cross-bridge kinetics. Dantzig et al. (Dantzig, J.A., N.J. Carter, J.C. Sparrow, D.C.S. White. 1992. *FASEB. J.* 6:A268) showed that mild treatment of *Lethocerus* IFM with calpain, which preferentially digests TnH in myofibrils (Bullard et al., 1988), resulted in a reduced amplitude of stretch activated tension. However, it is not understood how the TnH isoforms might act to translate stretch into enhanced cross-bridge binding. It is possible that the large proline rich extension of TnH mentioned above may link the thin and thick filaments and modulate the position of regulatory proteins, such as tropomyosin on the thin filament or myosin light chain 2 on the thick filament, in response to stretch (Tohtong et al., 1995).

The sophisticated genetic, molecular and mechanical manipulations possible in *Drosophila* make the fly a powerful system for investigating the structural and functional role of the tropomyosin isoforms in striated muscle (Fyrberg and Beall, 1990; Peckham et al., 1990; Sparrow et al., 1991). *Drosophila* tropomyosins are encoded by two closely linked third chromosome genes, *TmI* and *TmII*. Transcripts from both genes are alternatively spliced to produce protein isoforms expressed in different temporal and spatial patterns (Basi and Storti, 1984; Basi and Storti, 1986; Karlik and Fyrberg, 1986; Hanke and Storti, 1988). The two 284–amino acid protein isoforms encoded by *TmI*, Scm-TmI and Ifm-TmI, differ in only their COOH-terminal 27 amino acids (Basi et al., 1984; Basi and Storti, 1986). Scm-TmI is expressed in larval, adult head and abdominal muscles (Mogami et al., 1982; Basi et al., 1984). Ifm-TmI is expressed in the IFM and in the jump muscle (TDT) (Mogami and Hotta, 1982). *TmII* encodes two IFM-specific TnH isoforms, TnH-33 and TnH-34 (using the nomenclature of Cripps and Sparrow, 1992), a cytoplasmic isoform, and a muscle specific isoform (mTmII).

Ifm(3)3 is the only reported mutation in the *Drosophila TmI* gene (Mogami and Hotta, 1981; Karlik and Fyrberg, 1985). It is a dominant flightless *TmI* mutation due to the reduction in Ifm-TmI expression (Miller et al., 1993). Polymorphisms in the *TmII* gene have been identified (Cripps and Sparrow, 1992), as have mutations which affect the cytoplasmic isoform (Erdelyi et al., 1995); however, no mutations which affect muscle function have been identified in *TmII*. Here we show four mutations, TmI^{C10}, TmI^{J8}, TmI^{L2}, and TmI^{S2}, previously identified as the dominant flightless complementation group *l(3)nc99Eb* (Warmke et al., 1989), are alleles of the *TmI* gene, and identify a deletion, $Df(3R)ea^{5022}/TM3$ which uncovers both *TmI* and *TmII*. TmI^{C10} and $Df(3R)ea^{5022}/TM3$ represent the first molecularly defined deletions of the tropomyosin genes in *Drosophila*.

Here we show that deleting one copy of *TmI* has more deleterious effects than deleting one copy of *TmII* on flight behavior, wing beat frequency, myofibrillar organization, and dynamic stiffness and net power output of isolated single IFM fibers. Although our results indicate that the *TmII* isoforms TnH-33 and -34 are structural proteins in the IFM, power output of single fibers from a *TmII* heterozygote was only slightly decreased compared to wild-type. However, in extreme mutants of *TmI*, IFM severely depleted of Ifm-TmI (e.g., $TmI^{C10}/Ifm[3]3$ transheterozygotes) produced no net power. These results indicated that a reduction in the Ifm-TmI isoform to low levels not only disrupts the peripheral structure of IFM myofibrils, but also prevents the formation of force-generating cross-bridges between myofilaments.

Materials and Methods

Fly Stocks and Culture Conditions

The TmI^{C10} mutation was isolated by Roger Karess (C.N.R.S., Gif-Sar-Yvette, France) in a P–M hybrid dysgenic screen for embryonic recessive lethal mutations. The TmI^{J8}, TmI^{L2}, and TmI^{S2} mutations were induced by ethylmethane sulfonate (EMS) and isolated in screens for recessive lethal mutations of the myosin light chain 2 (*Mlc2*) gene (Warmke et al., 1989). Thus, these mutants initially appeared to be *Mlc2* alleles, but did not map to the *Mlc2* locus. The apparent interaction between TmI^{J8}, TmI^{L2}, TmI^{S2} and the *Mlc2* locus suggested *TmI*, and *Mlc2* interact; however, we have been unable to reproduce this effect. The dominant flightless, homozygous viable *TmI* mutant *Ifm(3)3* (Mogami and Hotta, 1981) has been characterized previously (Karlik and Fyrberg, 1985; Tansey et al., 1987; Molloy et al., 1992; Miller et al., 1993) and the stocks *w;Ifm(3)3* and the P[TmI^{+}] transformant line 10-2 (Tansey et al., 1987) were kindly provided by R. Storti (University of Illinois, Chicago, IL). The $Df(3R)ea^{5022rxl}$, *mwh e* deletion is an x-ray revertant of a dominant gain-of-function *easter* mutant ea^{5022} (Erdelyi and Szabad, 1989). This deletion was kindly provided by K.V. Anderson (Memorial Sloan Kettering Cancer Center, New

York). Third chromosome balancers used are *In(3LR)TM3, ri p^p sep su(Hw)^2 Sb bx^34e e, In(3LR)TM6B, Hu e Tb ca* (Craymer, 1984), and will be referred to as *TM3, Sb* and *TM6B, Tb*, respectively. Additional stocks and balancers used are described in Lindsley and Zimm (1992). Unless otherwise indicated, all fly stocks and crosses were maintained on cornmeal-agar-molasses–based media at 22°C.

Rescue of the Dominant Flightless and Recessive Lethal Phenotypes

The P[*TmI*$^+$] transformed line 10-2 (Tansey et al., 1987) carries the wild-type *TmI* gene on the X chromosome and was used to test for the rescue of the flightless and lethal phenotypes of *TmI*^{C10}, *TmI*^{J8}, *TmI*^{L2}, *TmI*^{S2}, and *Df(3R)ea*^{5022}. The P[*TmI*$^+$] transgene was introduced into Tm mutant heterozygotes (e.g., P[*TmI*$^+$]; *TmI*^{C10} *e*^{s}*/TM3, eSb*) and the flies were tested for flight rescue and the wing beat frequency measured. *Canton-S* control flies were also tested for flight ability and wing beat frequency. For lethal rescue, separate lines were established for *TmI*^{C10}, *TmI*^{J8}, *TmI*^{L2}, *TmI*^{S2}, and *Df(3R)ea*^{5022} in which all wild-type X chromosomes in mutant heterozygote males and females were replaced with the P[*TmI*$^+$] X chromosome. Crosses between the transformed lines were performed to determine if the number of copies of P[*TmI*$^+$] affected the viability of the *Tm* mutants over the deficiency (e.g., P[*TmI*$^+$];*TmI*^{C10} *e*^{s}*/Df(3R)ea*^{5022}).

Flight Testing and Wing Beat Frequency Analysis

Flight tests and wing beat analysis were performed as described (Warmke et al., 1992). Frequency components of wing beats were extracted by spectral analysis of light signal fluctuations (Hyatt and Maughan, 1994).

Identification of the Df(3R)ea^{5022} Breakpoints

Df(3R)ea^{5022}*/TM3, Sb* males and females were mated in small fly cages with attached yeast-seeded agar-grape plates. After a 1-h collection at 22°C, the plates were incubated for 20–24 h at 22°C and embryos were randomly selected from the plates and transferred to a 4 × 6 cm nitrocellulose filter. Each embryo was placed in a small circle that had been drawn on the filter by pencil. The embryos were punctured with a plastic pipet tip. The filter was processed according to standard bacterial colony hybridization protocols, except that the DNA was denatured for 15 min. Filters were hybridized with overlapping genomic DNA fragments isolated in a chromosome walk of the 88F region (Karlik et al., 1984) kindly supplied by E. Fyrberg (Johns Hopkins University, Baltimore, MD). DNA from the phage TML52, TML47, TML31, TML16, TM1, TMR16, TMR325, and TMR56, were labeled by nick translation with α-[^{32}P]deoxycytidine (Amersham Corp., Arlington Heights, IL) to a specific activity of 5–10 × 10^7 dpm. Prehybridization and hybridization with 10% dextran sulfate were done as described previously (Mullins et al., 1978). Genomic DNA isolated from *Df(3R)ea*^{5022}*/TM3, e Sb Ser*, and *Canton-S* was analyzed by genomic Southern analysis according to standard methods (Southern, 1975). *Canton-S* DNA was used as a control because the *mwh e* parental DNA was not available. Genomic DNA was transferred to a nylon membrane (Zeta-Probe from Bio-Rad Laboratories, Boston, MA or Nytran from Schleicher & Schuell, Keene, NH) by capillary action and probed with purified DNA fragments that were radio-labeled by random priming (Random Prime Labeling kit; United States Biochemical, Cleveland, OH) with α-[^{32}P]deoxycytidine. Prehybridizations and hybridizations were done at 65°C and high stringency washes were used to remove unbound probe.

Cloning of the TmI^{C10}, TmI^{J8}, TmI^{L2}, and TmI^{S2} Alleles

DNA from *TmI*^{C10}, *TmI*^{J8}, *TmI*^{L2}, and *TmI*^{S2} was analyzed by Southern analysis as described above. To clone the *TmI* alleles, genomic DNA was isolated from unhatched *Tm* mutant embryos, e.g., *TmI*^{C10}*/Df(3R)ea*^{5022} using a standard micromethod procedure. *Tm* mutant embryos develop to the embryo/larval boundary (~24 h at 22°C) but cannot hatch from the eggshell and were selected from a cross between *TmI*^{C10}, *TmI*^{J8}, *TmI*^{L2}, and *TmI*^{S2} heterozygotes and the deficiency *Df(3R)ea*^{5022}/+. Control *Canton-S* genomic DNA was prepared using the large scale preparation described previously (Falkenthal et al., 1984). Isolated *Canton-S* and *mutant/ea*^{5022} DNA was glass purified (USBioclean, United States Biochemical) and *TmI* sequences were amplified using PCR (Saiki et al., 1985) for 35 cycles (1 cycle = segment 1: 94°C, 1 min, segment 2: 45°C, 2 min, segment 3: 72°C, 3 min). The primer sequences used to amplify *TmI*^{J8}, *TmI*^{L2}, and *TmI*^{S2} sequences were: GCGAATTC**CAGCATACTCATTTGTATTATTTGG**′ and GCGGATCC**TGTCAGGGGCGTAGGAAGTTGGATA.** Oligonucleotide primers used to amplify *TmI*^{C10} sequences were: GCGAATTC-**GCAGACAGACACCTGCCTGTCACAC**; and GCGGATCC**TACAATAAGGCCTCGATTTGCGGAT.** The nucleotides in bold are *TmI* sequences, and the underlined nucleotides are EcoRI and BamHI restriction sites. *TmI*^{C10} amplification followed the same protocol as above, except that the enzyme was added after the denaturation temperature (94°C) had been reached (Mullis, 1991). All PCR amplified fragments were cloned into BluescriptKS+ (Stratagene Corp., La Jolla, CA) and three clones for each mutant were sequenced using the dideoxy termination method (Sanger et al., 1987).

Electron Microscopy

Adult IFM from 3–5-d-old flies was prepared for microscopy as described in Warmke et al. (1992) except that thoraces were fixed overnight at 4°C and post-fixed in 1% osmium tetroxide buffered with 0.1 M sodium phosphate, pH 7.2, for 1 h on ice in the dark. After fixation, IFM fibers were gently removed from the thoraces for embedding.

Protein Isolation and Analysis

For one-dimensional SDS-PAGE analysis of IFM myofibrillar proteins, muscles from half thoraces (12 half thoraces/genotype) were permeabilized in 50% glycerol buffer (20 mM sodium phosphate, pH 7.0, 1 mM NaN_3, 1 mM DTT, 2 mM $MgCl_2$, 50% glycerol, 0.5% Triton-X-100) for 1–2 d at −20°C. IFM fibers were dissected from half thoraces, transferred to homogenization buffer (100 mM NaCl, 10 mM sodium phosphate buffer, pH 7.0, 2 mM EGTA, 2 mM $MgCl_2$, 0.1 mg/ml soybean trypsin inhibitor, 1 mM DTT, 0.1 mM PMSF, 0.5% Triton-X-100), pelleted at 14,000 rpm, and then resuspended in homogenization buffer (10 μl/thorax). Pelleting and resuspension of the IFM were repeated twice, and then another three times in homogenization buffer without Triton X-100. The muscle pellets were then resuspended in SDS sample buffer, boiled for 5 min, and loaded on a 6% SDS-PAGE gel. Gels were stained with Coomassie blue (0.1% in 10% methanol, 10% acetic acid) and destained in 10% methanol, 10% acetic acid. Quantification of proteins was determined using a ScanMaker IISP (Microtek) and MacBas v. 2.31 quantitation software (Fuji Photo and Film, Ltd, and Kohshin Graphic Systems).

Preparation of Isolated IFM Fibers

Dorsal longitudinal fibers of the IFM, isolated from 2–5-d-old females which had been flight and wing beat tested, were dissected from split thoraces that were immersed for at least 1 h at 12°C in relaxing solution (~pCa 8, 5 mM MgATP, 15 mM creatine phosphate, 240 U/ml creatine phosphokinase [unless otherwise indicated], 1 mM free Mg^{2+}, 0.11 mM $CaCl_2$, 5 mM EGTA, and 20 mM BES, buffer, pH 7.0). Ionic strength was adjusted to 175 mM with added K or Na methyl sulfonate containing 50% (wt/vol) glycerol and a nonionic detergent, either 0.5% wt/vol Triton X-100 or 50 μg/ml saponin. Both types of detergents solubilize cellular membranes permitting equilibration of the bathing media with the interfilament spaces of the IFM (Maughan and Godt, 1989). 50 mM sucrose was included to prevent or reduce osmotic swelling of the mitochondria and sarcoplasmic reticulum. Skinning solutions contained Na methyl sulfonate, rather than K methyl sulfonate, to prevent depolarization of the membrane at the outset.

Freshly skinned fibers or skinned fibers which had been stored frozen (−50°C) up to 2 wk in relaxing solution (containing 50% (wt/vol) glycerol and 10 μg/ml leupeptin) were used for the mechanics. Aluminum T-clips were attached to the ends of the skinned fiber and the fiber transferred to a 30-μl drop of relaxing solution in a temperature controlled chamber filled with 0.5 ml mineral oil. Oil temperature was maintained at 12 ± 0.5°C by a Peltier device (Cambion; Cambridge Thermionic Corp., Cambridge, MA). One end of the fiber was attached via a T-clip to a strain gauge (AE801; SensoNor, Horten, Norway), the other end to a piezoelectric motor (P173; Physik Instrumente GmbH & Co., Waldbronn, Germany), and the fiber was stretched until just taut (zero stress). The relative position of the motor head was monitored by a variable impedance displacement transducer (KD-2310; Kaman Instrumentation Corp., Colorado Springs, CO). The fiber length (L, between the T clips) and the fiber width (at the narrowest part of the segment) were measured using a filar micrometer. The fiber was stretched incrementally (by 2.5–5% steps), to a final strain of 1.10–1.15 L (corresponding to a stress of ~1 kN m^{-2}). With each stretch, the force trace was allowed to return to a steady elevated level which followed a transient peak (i.e., the fiber was allowed to un-

dergo "stress relaxation"). Force was normalized to fiber cross-sectional area to correct for differences in fiber size. Fiber tension (in kN m^{-2}) was calculated by dividing force by fiber cross-sectional area, assuming a circular cross-section (unless otherwise indicated) by taking fiber width as the diameter. Analogue displacement and tension signals were monitored by a strip chart recorder with high-gain amplifier (WR3101; Watanabe Corp., Costa Mesa, CA), and a digital storage oscilloscope (2201; Tektronix Corp., Beaverton, OR).

Skinned fibers were activated incrementally by Ca^{2+} by exchanging equal volumes of pCa 8 relaxing solution for pCa 4.5 activating solution to attain pCa of 7, 6, and 5. Activating solutions had the same ionic composition as relaxing solution, except the total concentration of $CaCl_2$ was 5.03 mM (pCa 4.5) or 5.29 (pCa 4.0). Rigor was induced by exchanging activating solution for ATP-free (rigor) solution containing 5.03 mM $CaCl_2$ (pCa 4.5), 5 mM EGTA, 20 mM BES buffer (pH 7.0), and 175 mM ionic strength (adjusted with K methane sulfonate). At the end of each experiment, each fiber was fixed for light or electron microscopy by exchanging half the rigor solution volume with rigor solution containing 1% (wt/vol) gluteraldehyde. Solutions were formulated by solving a set of simultaneous equations describing the multiple equilibria of ions in the solutions (Godt and Lindley, 1982; Andrews et al., 1991).

Sinusoidal Analysis

Sinusoidal analysis (Zhao and Kawai, 1993) was used to determine the dynamic stiffness and power output of isolated muscle fibers. In this analysis, the length of a stretched skinned fiber was oscillated sinusoidally and the resultant force signal was measured and compared to the length signal to determine the complex stiffness of the fiber. The complex stiffness data were normalized for fiber dimensions to obtain the complex modulus. The complex modulus data obtained for each fiber were summarized graphically using Nyquist plots (Figs. 6–7), the abscissa and ordinate of which represent the elastic and viscous modulus respectively (Kawai and Brandt, 1980).

A strip of latex membrane (Trojan-enz; Carter-Wallace, New York) was used as a reference material to characterize and subtract the response of the apparatus (Kawai and Brandt, 1980).

Sinusoidal length pertubations of 0.25% fiber length (peak-to-peak) and 0.5–1,000 Hz were applied at 47 discrete frequencies (see Table III) using a microcomputer (486DX4-100 MHz microprocessor; ZEOS International, Inc., Minneapolis, MN) and a 16-bit data acquisition board (DT2838; Data Translation Inc., Marlboro, MA). The length and force signals from the servomotor and strain gauge were digitized, and the elastic modulus and viscous modulus components of the complex modulus were calculated by computing the amplitude ratio and the phase difference for tension and length at each frequency. Dynamic stiffness moduli (in N m^{-2}) were calculated as the vector sum of the elastic and viscous modulus at a given frequency. Power output (in watts) was calculated from the viscous modulus, the amplitude and frequency of the length perturbation, and the fiber cross-sectional area and length (see Table II caption for formulae). Details of the experimental setup and method of data acquisition are available upon request.

Results

The *Df(3R)ea^{5022}* Deletion Removes Both the *TmI* and *TmII* Genes

The *Df(3R)ea^{5022}* mutant is an x-ray induced revertant of the dominant *ea^{5022}* allele. Unlike easter mutants, *Df(3R)ea^{5022}* also shows a dominant flightless phenotype, suggesting an additional mutation is present on the *Df(3R)ea^{5022}* chromosome. The *Df(3R)ea^{5022}* chromosome has no cytologically visible deletion or rearrangement, but as the tropomyosin genes are located ~20-kb centromere proximal to the *easter* gene, a small deletion encompassing *easter* and the *Tm* genes might be cytologically invisible. We developed a novel technique to determine the extent of the *Df(3R)ea^{5022}* deletion and to test whether the deletion included the *Tm* genes.

Embryos obtained from a laying stock of *Df(3R)ea^{5022}* heterozygotes were hybridized with genomic phage from a walk which spanned the 88EF region (Fig. 1). DNA deleted in *Df(3R)ea^{5022}* was identified by the failure of specific clones to hybridize to one-quarter of the embryos (i.e., *Df(3R)ea^{5022}/Df(3R)ea^{5022}* embryos). DNA corresponding to the clones TML31, TML16, TM1, TMR16, and TMR325 was deleted in *Df(3R)ea^{5022}* (Fig. 1), a region that includes both tropomyosin genes, *TmI* and *TmII*. Genomic Southern analysis using *Df(3R)ea^{5022}* DNA showed the leftmost breakpoint was in the TML47 clone, indicating the *Df(3R)ea^{5022}* deletion removed all of the protein coding sequences of *TmII* (Fig. 2). Additional Southern analysis of *Df(3R)ea^{5022}* DNA using clones TMR16, TMR325, and TMR56 further showed the deletion extends centromere distal of the *TmI* and *easter* genes (data not shown; see Fig. 1). From these data, *Df(3R)ea^{5022}* deleted ~60 kb, including the *easter*, *TmI*, and *TmII* genes, but did not delete the IFM-specific actin gene, *Act88F*.

Rescue of Mutant Phenotypes by *TmI^{+}*

Genetic analysis showed the flightless and lethal phenotypes of four flightless alleles *C10*, *J8*, *L2*, and *S2* (Warmke et al., 1989) mapped to the interval uncovered by the *Df(3R)ea^{5022}* deletion (data not shown). *TmI* and *TmII* are the only myofibrillar protein genes in this region (Karlik et al., 1984), suggesting that *C10*, *J8*, *L2*, and *S2* were alleles of *TmI* and/or *TmII*. To determine if the mutants were *TmI* alleles, we attempted to rescue the flightless and lethal phenotypes using a transformed wild-type copy of the *TmI* gene (P[*TmI^{+}*]) introduced into the mutants by genetic crosses (see Materials and Methods). We assayed the flight behavior and wing beat frequency of each mutant heterozygote in the presence of the P[*TmI^{+}*] transgene, and determined if P[*TmI^{+}*] was able to rescue the recessive lethality of *mutant/Df(3R)ea^{5022}* flies. We tested for flight and lethal rescue in females since the X-linked P[*TmI^{+}*] gene is not fully dosage compensated in males (Tansey et al., 1987). The results showed both the flightless behavior and recessive lethality of *C10*, *J8*, *L2*, and *S2* were completely rescued to wild-type levels by the introduction of P[*TmI^{+}*] (Table I), indicating that *C10*, *J8*, *L2*, and *S2* were alleles of the *TmI* gene. Therefore, these alleles will be referred to hereafter as *TmI^{C10}*, *TmI^{J8}*, *TmI^{L2}*, and *TmI^{S2}*.

The flightless behavior of the *Df(3R)ea^{5022}* deletion was also rescued by P[*TmI^{+}*] (Table I), an unexpected result because P[*TmI^{+}*];*Df(3R)ea^{5022}/TM3* flies were still haploid for the *TmII* gene. The IFM is sensitive to the gene dosage of most contractile protein genes and perturbation in the IFM protein stoichiometry caused by mutation often results in a flightless phenotype (reviewed in Bernstein et al., 1993). However, our data indicated that, unlike the *TmI* gene, haploidy of the *TmII* gene reduced the wing beat frequency by ~20% but did not cause flightless behavior. The recessive lethality of *Df(3R)ea^{5022}* was not rescued by P[*TmI^{+}*], most likely because *TmII* is an essential gene (Erdelyi et al., 1995).

Molecular Analysis of the TmI Alleles

Genomic Southern analysis indicated no gross DNA rearrangements in *TmI^{J8}*, *TmI^{L2}*, or *TmI^{S2}*; however, a ~3.0-kb

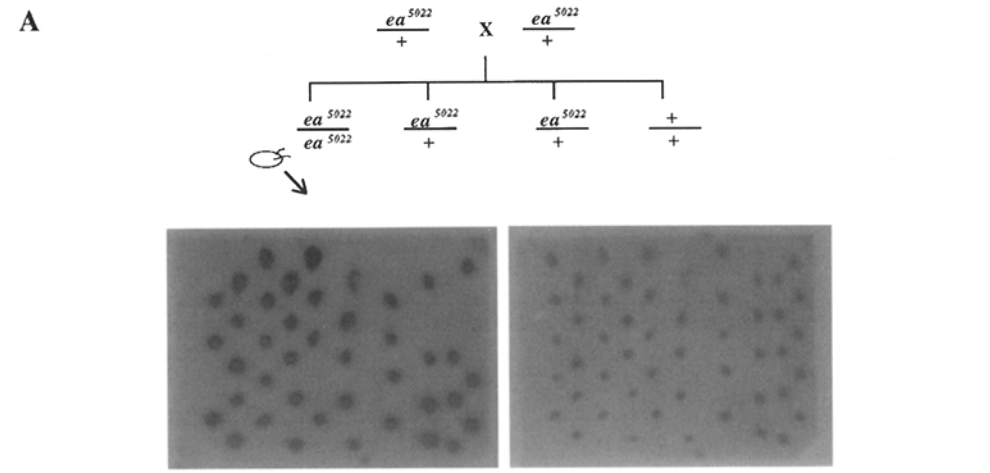

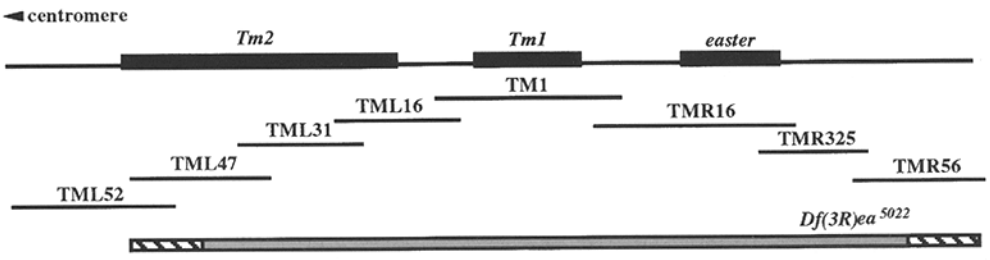

PHAGE	NUMBER OF EMBRYOS	OBSERVED HYBRIDIZATION	DNA DELETED
TML52	20	20	NO
TML47	20	20	NO
TML31	30	24	*YES*
TML16	24	20	*YES*
TM1	20	11	*YES*
TMR16	22	16	*YES*
TMR325	49	36	*YES*
TMR56	49	49	NO

Figure 1. $Df(3R)ea^{5022}$ deletes the *TmI*, *TmII*, and *easter* genes. (*A*) Embryos from the diagrammed cross were placed onto nitrocellulose filters, punctured, and hybridized with overlapping genomic clones from the 88EF region. A separate filter was used for each clone. The autoradiogram on the left is a filter hybridized with clone TMR325, while the right one is the same filter stripped and reprobed with a myosin light chain-2 genomic clone (cytological position 99D2-3) for a positive control. Embryos which did not hybridize to TMR325, but did hybridize to *Mlc2*, indicates DNA represented in TMR325 is deleted in $Df(3R)ea^{5022}$. (*B*) Summary of embryo hybridizations. The arrangement of the *TmI*, *TmII*, and *easter* genes on the third chromosome is diagrammed on the top line, and the eight overlapping genomic clones, TML52, TML47, TML31, TML16, TM1, TMR16, TMR325, and TMR56 are diagrammed below. The stippled bar indicates the minimal extent of the deletion in $Df(3R)ea^{5022}$, while the hatched bars represent the deletion breakpoint regions. These data are summarized in the table, showing that ~60 kb of DNA is deleted, including *TmI*, *TmII*, and *easter*.

deletion in the middle of the *TmI* gene was detected in TmI^{C10}. DNA isolated from $TmI^{C10}/Df(3R)ea^{5022}$ embryos was amplified using PCR and sequenced. The results indicated that the deletion breakpoints of TmI^{C10} are in introns 1 and 4 of *TmI*; consequently, exons 2, 3, and 4 are completely deleted (Fig. 3). These three exons encode all 284 amino acids of the IFM-specific *TmI* isoform and 257/284 of the amino acids in the embryonic *TmI* isoform. A muscle specific enhancer located in the first intron (Schultz et al., 1991; Gremke et al., 1993) is also deleted in TmI^{C10}. Therefore, TmI^{C10} is a null mutation of the *Drosophila TmI* gene.

We sequenced exons 2 and 3, common to the Scm-TmI and Ifm-TmI isoforms, in TmI^{J8}, TmI^{L2}, and TmI^{S2} to search for mutations which must lie in this region as the mutants are both embryonic lethal and flightless. The results indicated that all three mutants contained single base changes in exon 2 of *TmI* (Fig. 3). Both TmI^{J8} and TmI^{L2} contained nonsense mutations, while TmI^{S2} resulted in a missense mutation (Asn for Asp121). These base changes in TmI^{J8}, TmI^{L2}, and TmI^{S2} were the only mutations detected in three individual clones isolated from each mutant allele. All three mutations are located in the second exon; consequently, each affects both the IFM-specific and -embryonic isoforms of *TmI*, consistent with the flightless and lethal phenotypes of the mutants.

Myofibrillar Structure of Tropomyosin Mutant IFM

To determine the effect of reduced Ifm-TmI and TnH-33/34 accumulation on IFM assembly and ultrastructure, we compared electron micrographs of intact IFM from the tropomyosin mutants and wild-type flies. The ultrastructure of the four single *TmI* mutants, TmI^{C10}, TmI^{J8}, TmI^{L2}, and TmI^{S2} were indistinguishable from each other; therefore, only representative micrographs are shown from this group.

Cross-sections showed the myofibrillar lattice of *TmI* single heterozygotes (e.g., $TmI^{C10}/+$) was well preserved at the core, but was disrupted around the fibril periphery

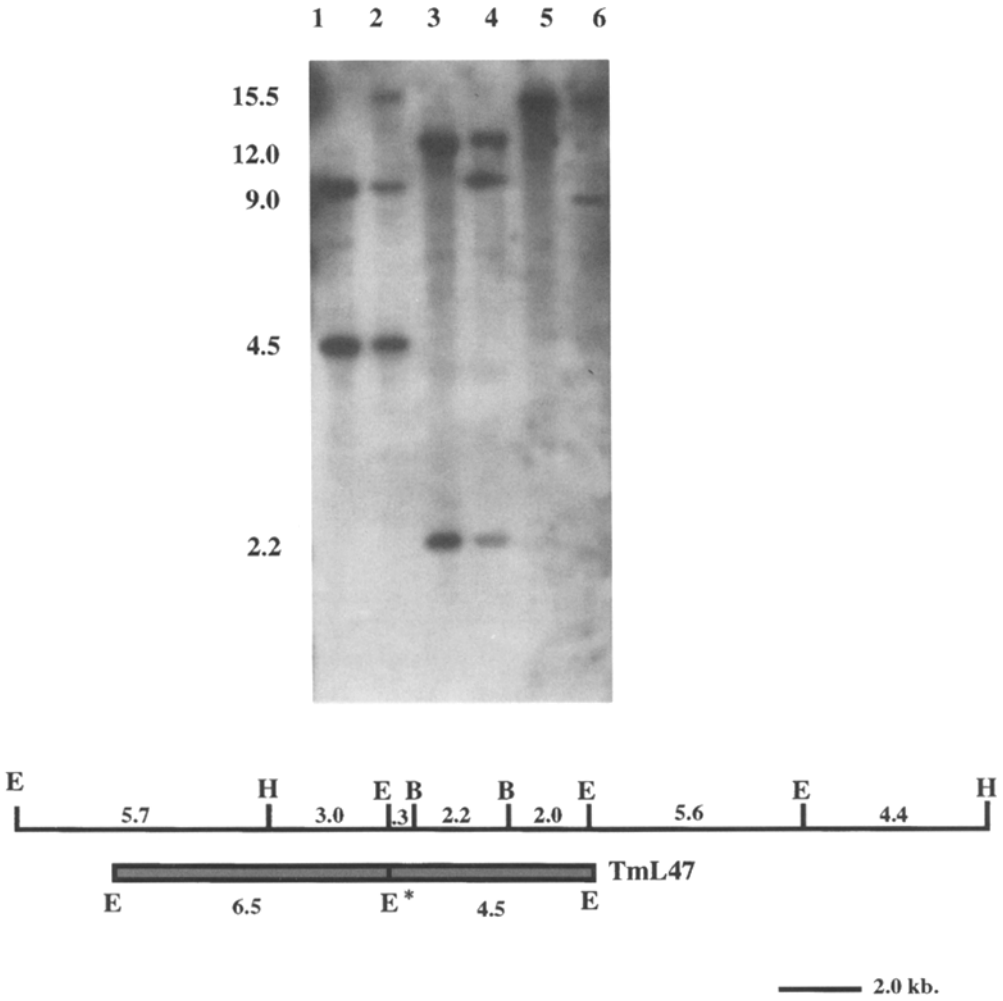

Figure 2. Southern analysis showed the *TmII* coding region is deleted in *Df(3R)ea*^{5022}. Odd numbered lanes are wild-type control DNA (+/*TM3, e Sb*); even numbered lanes are *Df(3R)ea*^{5022}/*TM3, e Sb* DNA. DNA in lanes *1* and *2* was digested with EcoRI (*E*); lanes *3* and *4* with BamHI (*B*); lanes *5* and *6* with HindIII (*H*). A partial restriction map of the region is diagrammed below the autoradiogram. The 11.0-kb EcoRI fragment from TML47 (*shaded box*) hybridized to unique fragments in the *Df(3R)ea*^{5022} lanes. Further analysis indicated only the 6.5-kb EcoRI fragment of TML47 hybridized to the junction fragments (data not shown). Therefore, the left deletion breakpoint lies 5′ of the EcoRI site marked with an asterisk (*). This restriction site corresponds to an EcoRI site in the 5′ UTR of the *TmII* gene (Hanke and Storti, 1988).

(Fig. 4 *e*). The cylindrical shape was distorted compared to wild type as peripheral filaments detached from the main core. The number of thick filaments across the mid-line of a wild-type myofibril was 36 ± 1.0 (Fig. 4 *a*); however, the diameter of the *TmI* mutant myofibrils was reduced to ~25–27-thick filaments. Longitudinal sections of the mutant heterozygotes also showed alterations when compared to wild type. Wild-type myofibrils were straight and of constant width, with sarcomeres that were 3.3 ± 0.2 μm long and evenly spaced by Z bands (Fig. 4 *b*). The average length of the *TmI* mutant sarcomeres was similar to wild-type (3.2 ± 0.2 μm); however strands of thin and thick filaments splayed off from the fibril periphery giving it a frayed appearance (Fig. 4, *f* and *h*). Myofibrillar structure of rescued *TmI* mutants (e.g., P[*TmI*$^{+}$];*TmI*^{C10}/+) was similar to wild type in both longitudinal and cross-sections (data not shown, but see Table II).

The peripheral disruptions of myofibrils from *TmI*/*TmII* double heterozygotes (*Df[3R]ea*^{5022}/+) appeared similar to the four *TmI* single mutants in longitudinal and cross-sections, including the presence of detached filaments, but the hexagonal lattice core was consistently smaller, reduced to 21 ± 3.0-thick filaments (Fig. 4 *g*). Myofibrils from *TmII* single heterozygotes (P[*TmI*$^{+}$];*Df(3R)ea*^{5022}/+) (Fig. 4 *c*) also have fibrils with a smaller fibril diameter (31 ± 1.0 thick filaments) compared with wild type; however, peripheral filaments are neatly arranged in these mutant fibrils. To confirm that the smaller fibril diameter in P[*TmI*$^{+}$];*Df(3R)ea*^{5022}/+ IFM was due solely to mutation of *TmII* and not to reduced or weak expression of the transformed *TmI*$^{+}$ gene, we analyzed IFM ultrastructure from *Df(3R)ea*^{5022} flies with two copies of *TmI*$^{+}$. Fibrils from P[*TmI*$^{+}$]/P[*TmI*$^{+}$];*Df(3R)ea*^{5022}/+ flies were similar (32 ± 1.0 thick filaments) to those from P[*TmI*$^{+}$];*Df(3R)ea*^{5022}/+ flies. In addition, deletion of one copy of the *TmII* gene resulted in a corresponding reduction in the level of TnH protein in the IFM. We measured the relative level of TnH in wild type and P[*TmI*$^{+}$];*Df(3R)ea*^{5022}/+ heterozygotes using one-dimensional SDS-PAGE and gel scanning and quantitation (see Materials and Methods). The results indicated TnH protein levels were reduced ~40–50% in P[*TmI*$^{+}$];*Df(3R)ea*^{5022}/+ heterozygotes compared to wild type (data not shown), confirming that deletion of one copy of the *TmII* gene reduced IFM TnH protein levels and is likely the cause of the reduction in diameter of myofibrils in the *TmII* mutant IFM.

To assess the effect in more extreme tropomyosin mutants, we analyzed the IFM ultrastructure of the mutants transheterozygous with the hypomorph *Ifm(3)3* (*TmI*^{C10}/*Ifm[3]3*, *TmI*^{J8}/*Ifm[3]3*, *TmI*^{L2}/*Ifm[3]3*, *TmI*^{S2}/*Ifm[3]3*, and *Df[3R]ea*^{5022}/*Ifm[3]3*). Compared to the mutant heterozygotes, the most apparent structural effect was the drasti-

Table I. Rescue of Flightless Behavior and Lethality by P[TmI$^+$]

Allele	Flight index	Wing beat frequency (Hz)‡	Viability index§
Canton-S	6.5 ± 1.0	226.0 ± 13.0	—
TmI^{C10}/+	1.3 ± 2.0	141.3 ± 6.0	0.0
P[TmI$^+$];TmI^{C10}/+	5.1 ± 2.4	206.0 ± 7.0	100.0
TmI^{J8}/+	2.4 ± 2.3	153.3 ± 6.0	0.0
P[TmI$^+$];TmI^{J8}/+	6.3 ± 1.8	232.0 ± 4.0	76.0
TmI^{L2}/+	1.2 ± 1.7	138.3 ± 7.0	0.0
P[TmI$^+$]; TmI^{L2}/+	6.2 ± 1.7	223.0 ± 12.0	100.0
TmI^{S2}/+	0.4 ± 1.1	137.0 ± 9.0	0.0
P[TmI$^+$]; TmI^{S2}/+	5.5 ± 2.3	235.0 ± 11.0	100.0
Df(3R)ea^{5022}/+	0.3 ± 1.1	~0.0‖	ND
P[TmI$^+$]; Df(3R)ea^{5022}/+	5.4 ± 2.1	179.5 ± 5.0	ND

*Flight indices were determined by taking the mean (±SEM) of the individual scores of ~100 flies from each genotype using the flight test cylinder.
‡Wing beat frequencies were measured as described in the Materials and Methods. Approximately 5–10 flies from each genotype were tested.
§The percentage of expected transheterozygotes recovered from lethal rescue crosses described in Materials and Methods was determined. Approximately 100 progeny were scored for each cross.
‖*Df(3R)ea^{5022}* flies do not generate sustained wing beats.
ND, not determined.

cally reduced core size and increased severity of the peripheral disruptions (compare Fig. 4 *e* and Fig. 5, *a* and *c*). The diameter of the lattice core of the *TmI* transheterozygote fibrils was approximately one-half that of wild type, reduced to 16 ± 2.0 thick filaments. Abundant unattached thick filaments were scattered around the periphery of the fibrils, but fewer unattached thin filaments were seen. In longitudinal sections, fibrils tended to be thin and wavy compared to wild type, and the sarcomere lengths were shorter on average (e.g., 2.6 ± 0.2 μm for *TmI^{C10}/Ifm[3]3*, Fig. 5 *b*). Fibrils from *Df(3R)ea^{5022}/Ifm(3)3* transheterozygotes were structurally similar, but again, deletion of the *TmII* gene on the *Df(3R)ea^{5022}* chromosome augmented the disruption by reducing the core diameter to 13 ± 1.0 thick filaments (Fig. 5 *c*). Occasionally, fibrils from transheterozygotes contained sarcomeres with multiple, tandemly arrayed Z bands that often did not span the entire width of the fibril (see Fig. 5 *d*). Multiple Z bands have been reported for other *Drosophila* myofibrillar protein gene mutants (Reedy et al., 1989; Fyrberg et al., 1990; Sparrow et al., 1992), including the *TmI* hypomorph *Ifm(3)3* (Miller et al., 1993).

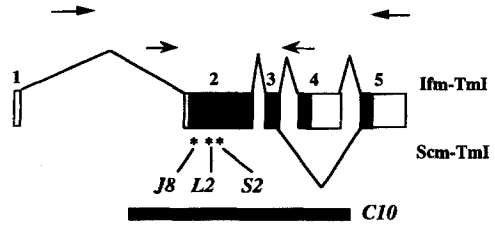

TmI Allele	Mutation
C10	**Deletion**
J8	**Gln28 > STOP**
L2	**Gln92 > STOP**
S2	**Asp121 > Asn**

Figure 3. *TmI^{C10}* is a *TmI* deletion and *TmI^{J8}*, *TmI^{L2}*, and *TmI^{S2}* are *TmI* point mutants. The exon–intron arrangement of the *TmI* gene is diagrammed showing the relative locations of the *TmI* mutations. The arrows above represent locations of oligonucleotides used to amplify *TmI^{C10}/Df(3R)ea^{5022}* embryo DNA using PCR, and the barbed arrowheads represent oligonucleotides used to amplify *TmI^{J8}*, *TmI^{L2}*, and *TmI^{S2}/Df(3R)ea^{5022}* DNA. *TmI^{C10}* deletes exons 2, 3, and 4 of *TmI* (*black bar*). *TmI^{J8}*, *TmI^{L2}*, and *TmI^{S2}*, denoted by asterisks, are all G>A transitions resulting in either nonsense mutations (*TmI^{J8}*, *TmI^{L2}*) or a missense mutation (*TmI^{S2}*).

Mechanical Analysis of Skinned Single Fibers

To determine the extent to which the reduced or absent wing beat frequency conferred by the tropomyosin mutants was associated with reduced or altered contractile properties of the flight muscles, we measured isometric tension, dynamic stiffness, and power output of Ca^{2+}- and stretch-activated skinned fibers, comparing responses from *TmI^{C10}/+* and *Df(3R)ea^{5022}/+* and *TmI^{C10}/Ifm(3)3* and *Df(3R)ea^{5022}/Ifm(3)3* with those from wild type and P[*TmI$^+$*];*TmI^{C10}/+* and P[*TmI$^+$*];*Df(3R)ea^{5022}/+* heterozygotes.

In skinned fibers from wild-type, elevating [Ca^{2+}] produced a sigmoidal increase in isometric tension, from pCa (= $-\log [Ca^{2+}]$) ~7 to a saturating maximum at pCa ~5 (12°C). The pCa for half maximum tension was ~6.3, the slope of the relationship at half maximum (the Hill coefficient: Warmke et al., 1992) was ~1.3, and the maximum isometric tension was 1.13 ± 1.0 kN/m^2 (pCa 5). Maximum isometric tension of fibers from P[*TmI$^+$*];*TmI^{C10}/+* (1.10 ± 1.1 kN/m^2), P[*TmI$^+$*]*Df(3R)ea^{5022}/+* (0.90 ± 0.6 kN/m^2), and *TmI^{C10}/+* (0.84 ± 0.7 kN/m^2) heterozygotes were on average lower than that of wild type, but the differences were not significant ($P > 0.05$). Maximum isometric tension of fibers from *Df(3R)ea^{5022}/+* (0.26 ± 0.1 kN/m^2) was significantly less than wild type ($P < 0.05$), as were those of *TmI^{C10}/Ifm(3)3* (0.31 ± 0.4 kN/m^2) and *Df(3R)ea^{5022}/Ifm(3)3* (0.05 ± 0.1 kN/m^2).

Changes in muscle force produced by the fibers in response to length pertubations were measured using rapid sinusoidal oscillations (Kawai and Brandt, 1980). Fibers were oscillated at different frequencies (including that for optimal power generation in Ca^{2+}-activated fibers) under

Figure 4. Electron micrographs of *TmI*, *TmII*, and *TmI/TmII* heterozygotes. Transmission electron micrographs of adult *Canton-S* (*a* and *b*); P[TmI^{+}];$Df(3R)ea^{5022}/TM3$ (*c* and *d*); $TmI^{C10}/TM3$ (*e* and *f*); and $Df(3R)ea^{5022}/TM3$ (*g* and *h*) indirect flight muscles. The left-hand panels of myofiber transverse sections show an ordered myofilament lattice of myofibrils, 35–36 thick filaments across in wild-type (*a*), that is maintained in a *TmII* mutant myofibril (*c*), although decreased in diameter to 31–32 filaments. In contrast, *TmI* (*e*) and *TmI/*

Table II. Summary of In Vivo and In Vitro Mechanical and Ultrastructural Data from TM⁻ Mutant Strains

Fiber genotype	In vivo							In vitro single IFM					
	TmI Copy No.	*TmII* copy No.	Flight index*	Wbf‡	Fraction of *CS*	Thick filament No.§	Fraction of *CS* area	Elastic modulus‖ ($N\ m^{-2}$)	Dynamic stiffness¶ ($N\ m^{-2}$)	Fraction of *CS*	Square root fraction of *CS*	Power output** (Wm^{-3})	Fraction of *CS*
				Hz									
1 *Canton-S*	2	2	6.5 ± 1.0	226 ± 13	1.00	35.5 ± 1.0	1.00	634 ± 70	689 ± 76	1.00	1.00	117 ± 23	1.00
2 *P[Tm1];TmI^{C10}*	2	2	5.13 ± 2.4	206 ± 7	0.91	35.5 ± 0.5	1.00	546 ± 121	568 ± 121	0.82	0.91	60 ± 20	0.60
3 *TmI^{C10}/TM3*	1	2	1.25 ± 2.0	141 ± 6	0.62	25.3 ± 2.2	0.51	338 ± 70	346 ± 73	0.50	0.71	38 ± 14	0.32
4 *TmI^{C10}/Ifm(3)3*	~0	2	~0	0	0	16.0 ± 2.0	0.20	79 ± 30	79 ± 30	0.11	0.34	−1 ± 1	<0.01
5 *P[Tm1];Df(3R)ea^{5022}*	2	1	5.4 ± 2.1	180 ± 5	0.80	32.3 ± 1.4	0.83	530 ± 83	554 ± 90	0.80	0.90	85 ± 25	0.73
6 *Df(3R)ea^{5022}/TM3*	1	1	0.33 ± 1.1	0	0	21.5 ± 2.6	0.37	391 ± 25	394 ± 26	0.57	0.76	26 ± 4	0.22
7 *Df(3R)ea^{5022}/Ifm(3)3*	~0	1	~0	0	0	13.0 ± 1.0	0.13	91 ± 18	92 ± 18	0.13	0.37	−1 ± 1	<0.01

Values are means and S.E.M; *N = 65–100; ‡N = 5–10; §N = 10–23; ‖¶**N = 4–7 flies. Copy No. refers to whether the strain is haploid or diploid with respect to the *TmI* or *TmII* gene. Flight index and wing beat frequency (*Wbf*) values, at 22°C, are taken from Table I. Fraction of CS refers to the fractional value with respect to that of wild type (*Canton S.*) Thick filament No. refers to the number of thick filament in the organized lattice across the diameter of a representative myofibril. Area refers to the cross-sectional area of the organized myofibrillar lattice, which is proportional to the thick filament number. ‖Elastic modulus refer to the IFM in-phase stiffness modulus at the frequency of peak power output (f_{max}, in s^{-1}), at pCa 5. ¶Dynamic stiffness refers to the vector sum of the elastic and viscous moduli at f_{max} at pCa 5. **Power output (in watts m^{-3} fiber volume) refers to maximum power output at pCa 5:2 $\pi\, f_{max}\, Ev\, ([\Delta L/L]_{rms})^2$, where E_v is the viscous modulus (kN/m²), $\Delta L/L$ is half the peak-to-peak amplitude of the sinusoidal length perturbation ΔL divided by the length of the muscle L, and *rms* is the root-mean-square of the perturbation amplitude. In the present experiments, $([\Delta L/L]_{rms})^2 = 0.5\ (0.00125)^2$. All single fiber mechanical measurements were conducted at 12°C. Pairwise comparison of values were conducted for the following combinations of strains: 2 vs. 1, 3 vs. 2, 4 vs. 3, 5 vs. 2, 5 vs. 3, 6 vs. 5, and 7 vs. 6. Significant differences ($P < 0.05$) were noted for the following combinations: *6 vs. 5. ‡3 or 5 vs. 2; 5 vs. 3. ‖¶**3,4,6, or 7 vs. 1; 4, 6, or 7 vs. 2, 4 vs. 3; 4 vs. 1; 7 vs. 6; all other combinations tested were not significantly different ($P > 0.05$).

conditions of relaxation, Ca^{2+} activation and rigor. Results were analyzed graphically as Nyquist plots (Figs. 6 and 7). Data obtained from the plots are summarized in Table II.

In the relaxed and rigor states, the amplitude of the dynamic modulus (the vector sum of the elastic and viscous moduli) increased as a function of frequency, but the phase remained roughly constant. This yielded a Nyquist plot that was roughly linear over the range of applied frequencies (0.5–1,000 Hz). In the active state, the Nyquist plot was looped, with pronounced phase shifts at intermediate frequencies that result from negative-going values of the viscous modulus. Negative-going values are due to actomyosin interactions that, in response to stretch, perform mechanical work on the apparatus. In the living fly this oscillatory work powers flight (Thorson and White, 1969).

The amount of work performed during each oscillation (and during each wing stroke) is proportional to the amplitude of the Nyquist loop, which varied considerably in size, being largest in wild type (not shown), P[*TmI*$^+$]; *TmI^{C10}*/+, and P[*TmI*$^+$]*Df(3R)ea^{5022}*/+ (Figs. 6 and 7, *A*), less in *TmI^{C10}*/+ and *Df(3R)ea^{5022}*/+ (Figs. 6 and 7, *B*), and almost absent in *TmI^{C10}/Ifm(3)3* and *Df(3R)ea^{5022}/Ifm(3)3* (Figs. 6 and 7, *C*). Power output was graded correspondingly (Table II). IFM net power output of P[*TmI*$^+$]; *TmI^{C10}*/+ and P[*TmI*$^+$]*Df(3R)ea^{5022}*/+ fibers was 60 and 73%, respectively (wild type = 100%). Power output dropped to 32% for *TmI^{C10}*/+, 22% for *Df(3R)ea^{5022}*/+ and < 0.01% for *TmI^{C10}/Ifm(3)3* and *Df(3R)ea^{5022}/Ifm(3)3* IFM fibers. Together with the flight behavior and wing beat frequencies of the mutants, these results suggested a power output of ~60% that of wild type (e.g., the power output of P[*TmI*$^+$];*TmI^{C10}*/+) may be near the minimum required for flight, consistent with the results of others (Laurie-Alberg et al., 1985; Tohtong et al., 1995). There also appears to be a threshold of power production below which a wingbeat is impossible. The results indicated that 32% power output was enough for a moderate wingbeat (~141 Hz) in *TmI^{C10}*/+ , but 22% power was not enough to even flap the wings in *Df(3R)ea^{5022}*/+ flies. We observed in *Df(3R)ea^{5022}*/+ (and in the transheterozygotes) that IFM fibers teased away from the thoracic cuticle more easily than in the other *Tm* mutants, suggesting that IFM attachment sites to the thorax are weak in *Df(3R)ea^{5022}*/+ and in the transheterozygotes. Therefore, the absence of wingbeats in these mutants may be the combined result of reduced or negligible power production from the IFM and weak attachment sites which do not transmit power from the IFM to the cuticle.

The active dynamic stiffness moduli of the mutant fibers (i.e., a rough measure of the number of crossbridges attached) at the frequency of maximum power (for *Canton-S*, 78 ± 12 s^{-1} at 12°C or 215 s^{-1} at 22°C, assuming a Q_{10} of 2.8 (Maughan D.W., unpublished results)) was reduced roughly in proportion to the extent to which the myofibril was disrupted (Table II; compare dynamic stiffness "fraction of CS" with myofibrillar fractional area disrupted). This suggested that the stiffness of the fibers resulted from actomyosin cross-bridges forming between filaments contained in the well-ordered cores of the mutant fibers, but not between disorganized filaments in the fibril periphery. Additionally, wing beat frequency correlated with the square root of dynamic stiffness. This result is consistent

TmII (*g*) mutant myofibrils are deformed as peripheral thick and thin filaments detach from the fibrils, leaving smaller cores with ~26 (*TmI*) and ~23 (*TmI/TmII*) thick filaments across. The longitudinal sections in the right panels show that sarcomere spacing in the mutant fibrils is similar to that in wild-type (~3.3 μm). Fibrils in *TmI* and *TmI/TmII* fibrils appear ragged as thick and thin filaments splay off and Z bands become wavy and out-of-register. Bars: (*a*, *c*, *e*, and *g*) 0.5 μm; (*b*, *d*, *f*, and *h*) 2.0 μm.

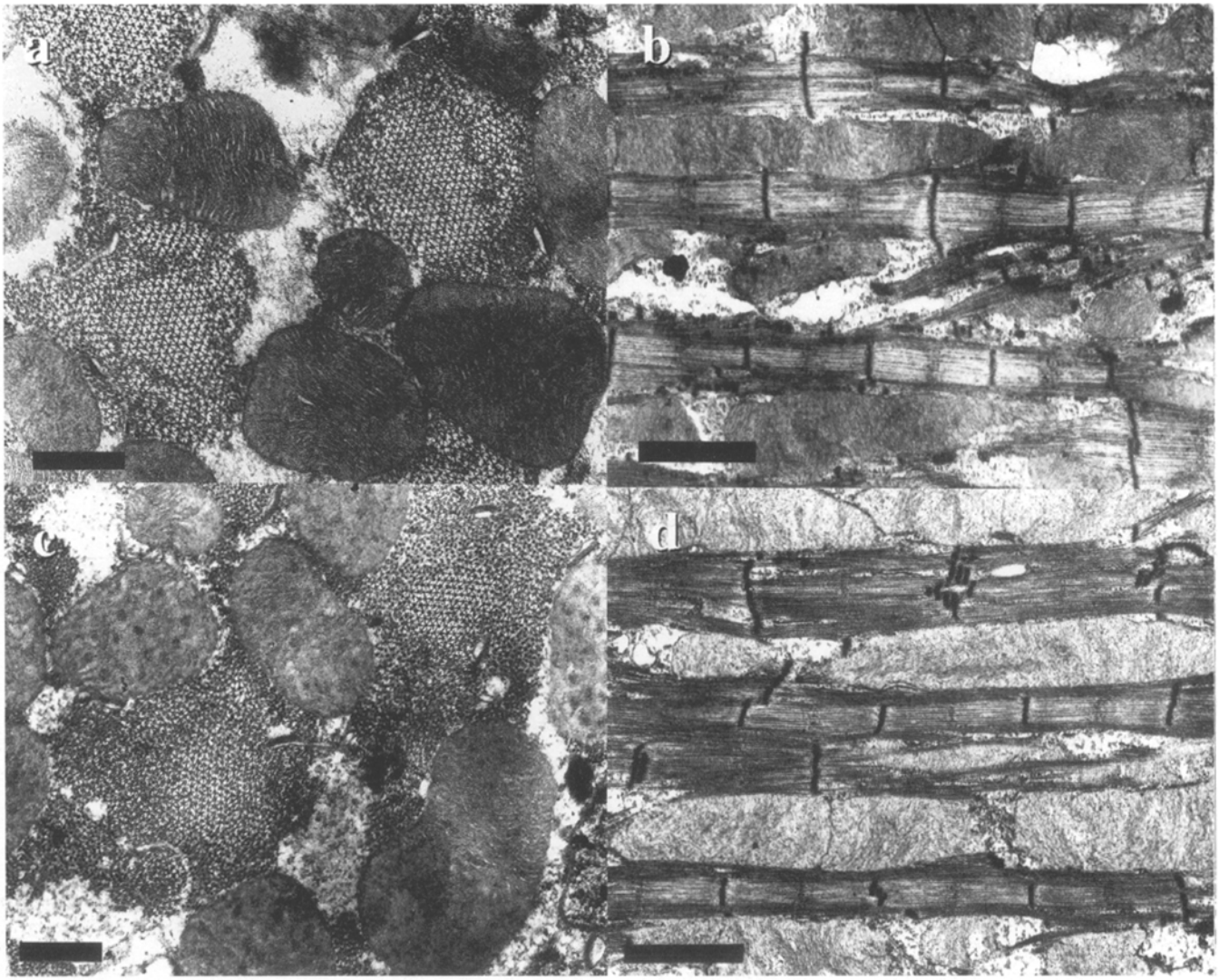

Figure 5. Electron micrographs of $TmI^{C10}/Ifm(3)3$ and $Df(3R)ea^{5022}/Ifm(3)3$ transheterozygotes. Transmission electron micrographs of adult $TmI^{C10}/Ifm(3)3$ (*a* and *b*) and $Df(3R)ea^{5022}/Ifm(3)3$ (*c* and *d*) indirect flight muscles. The transverse sections show the ordered myofilament lattice has decreased to 16–17 thick filaments across in $TmI^{C10}/Ifm(3)3$ and 12–13 across in $Df(3R)ea^{5022}/Ifm(3)3$ with many unattached thick filaments scattered in the fibril periphery. The longitudinal sections (*b* and *d*) show fibrils with short sarcomeres (~2.7–2.9 μm) bound by irregular Z disks which are sometimes split or tandemly arranged. Filaments often splay off from the fibril periphery in the transheterozygotes. Bars: (*a* and *c*) 0.5 μm; (*b* and *d*) 2.0 μm.

with other reports (Molloy et al., 1992; Tohtong et al., 1995) that suggest dynamic stiffness of the flight system resides primarily in the myofilaments and, as such, is a major determinant of wing beat frequency.

Discussion

Tropomyosin is a thin filament linked protein which has both a structural role in myofilament assembly and a regulatory role in muscle contraction. The fruit fly *D. melanogaster* provides a well-defined system to study the structural and regulatory roles of tropomyosin in the IFM. The three Drosophila tropomyosin isoforms expressed in the IFM, the Ifm-TmI isoform encoded by the *TmI* gene and the two IFM-specific TnH-33 and 34 isoforms encoded by *TmII*, are structurally similar except that the TnH isoforms contain an additional ~200 amino acid COOH-terminal domain. Previously, our mechanical analysis of the stretch activation properties of fibers from the hypomorphic *TmI* mutant, *Ifm(3)3*, showed that in muscle deficient in Ifm-TmI, crossbridges were not able to bind and actively cycle (Molloy et al., 1992). However, no *TmII* mutation which affects TnH function has been described; therefore, the role(s) of the TnH isoforms in the IFM was not clear. Here, using the first reported null mutants of the two *Drosophila* tropomyosin genes *TmI* and *TmII*, we set out to characterize further the individual and comparative roles of Ifm-TmI and TnH-33 and 34, focusing specifically on the structural roles of the Ifm-TmI and TnH-33 and 34 in the IFM and the stretch activation properties of muscle deficient in these tropomyosin isoforms.

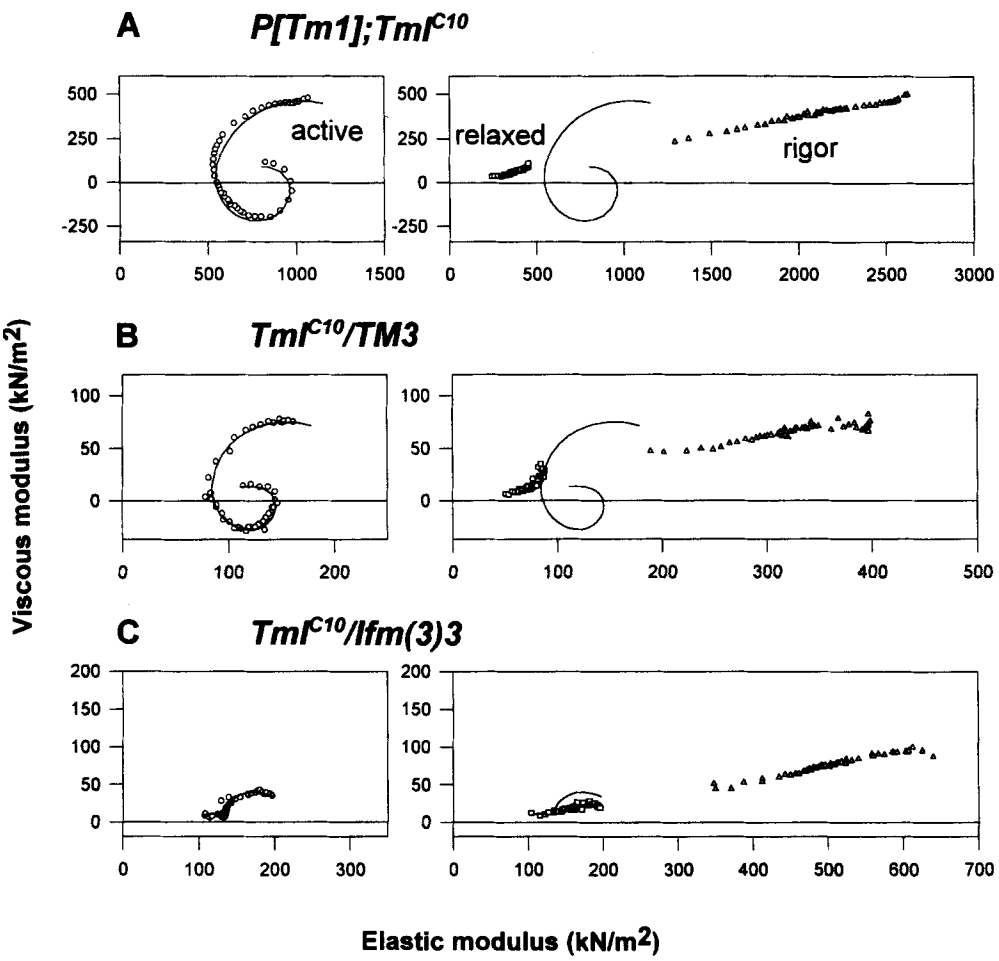

Figure 6. Nyquist plots of elastic modulus (abscissa) versus viscous modulus (ordinate) of skinned IFM fibers from *TmI* mutant lines. Experimental points, corrected for the characteristics of the apparatus, are plotted at 47 frequencies between 0.5 Hz and 1 kHz (left to right). Left panels represent data obtained from active fibers (pCa 5, *circles*). The solid curves are least squares fits to the data using a three-element viscoelastic model (Maughan, D.W., C. Hyatt, unpublished). Right panels represent the relaxed (pCa 8, *squares*) and rigor (*triangles*) data obtained from the same fibers. The active curves in the left panels are replotted for comparison. Note the progressive reduction in both viscous and elastic moduli and active loop size as the *TmI* gene copy number decreases from two ($P[TmI^+]$; $TmI^{C10}/+$) to one ($TmI^{C10}/+$), to essentially zero ($TmI^{C10}/Ifm[3]3$). Plots from wildtype flies were similar in appearance to that of $P[TmI^+];TmI^{C10}/+$. Also note the X axes vary in the figure parts.

Myofibrillar Assembly in IFM Reduced for Tropomyosin

Loss of function mutations in genes encoding many IFM-specific contractile proteins, such as myosin, actin, troponin, myosin light chain-2, and α-actinin have been identified based on their dominant flightless phenotype, and most often result in severe myofibrillar defects (reviewed in Bernstein et al., 1993). The *TmI* gene encodes the only standard tropomyosin isoform (Ifm-TmI) present in the IFM (Mogami et al., 1982); therefore, it was not surprising that mutations which affected this isoform, including the *TmI* alleles described in this report, resulted in severe fibrillar disruptions in the IFM (Karlik et al., 1985; Tansey et al., 1987; Miller et al., 1993; Figs. 4 and 5).

Ultrastructural analysis of myofibrillar assembly of wild-type IFMs, characterized in *Drosophila* by Shafiq (1963) and most recently by Reedy and Beall (1993), indicate the number of sarcomeres in an IFM myofibril is determined early in development and the growth of each fibril occurs by the addition of thin and thick filaments around the fibril periphery. This suggests the filaments at the core of the fibrils are laid down first and outer filaments are assembled later. Based on studies that showed thin filaments assembled without tropomyosin were destabilized in vitro (Hitchcock-Degregori et al., 1988; Broschat, 1990; Weigt et al., 1990;) and in vivo (Liu and Bretscher, 1989), Miller et al. (1993) proposed that a decrease in Ifm-TmI leads to fewer, or less stable, thin filaments available for myofibrillar assembly, resulting in myofibrils with normal lattice cores but unassembled thick filaments in the fibril periphery. One prediction of this hypothesis is that as the level of Ifm-TmI decreases, the size of the assembled lattice core shrinks as fewer thin filaments are available for incorporation. Our results from the IFM of the *TmI* heterozygotes and transheterozygotes supported this prediction. However, it was also evident that a reduction of Ifm-TmI to very low levels (3–4% that of wildtype is estimated in $TmI^{C10}/Ifm(3)3$, based on Ifm-TmI levels in *Ifm(3)3/Ifm(3)3* reported by Miller et al., 1993), did not have as severe an effect on the size of the lattice fibrillar core as that expected (cores reduced to only ~20% that of wild type). It is possible that the low level of Ifm-TmI in the transheterozygotes is sufficient to initiate thin filament assembly in the small fibril cores, but it does not appear that Ifm-TmI is absolutely required for the structural integrity of myofibrils.

There are other myofibrillar proteins which likely contribute to the stability and/or assembly of thin filaments in vivo, and which could maintain fibrillar structure by substituting for or replacing Ifm-TmI. One possibility is TnH-33 and 34, which have tropomyosin domains with actin binding sites, could bind actin and thereby stabilize thin filaments in the absence of Ifm-TmI. The fact that TnH-33

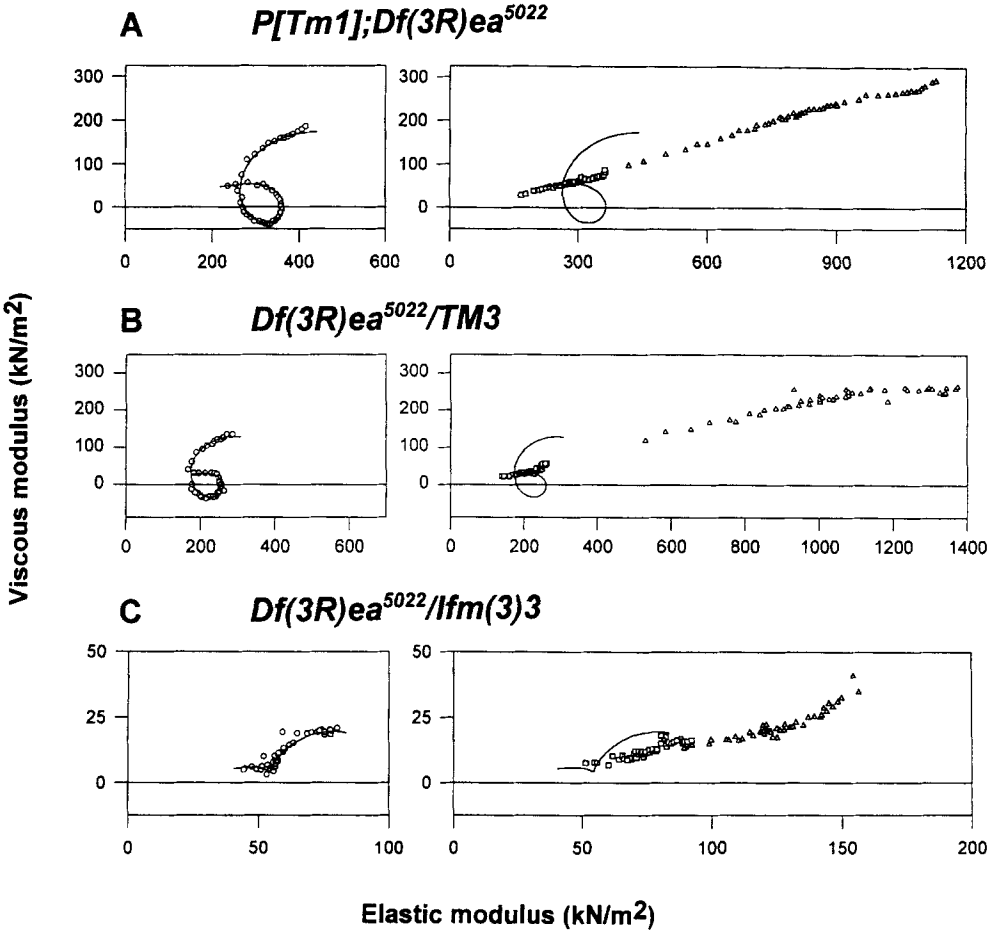

Figure 7. Nyquist plots of elastic modulus (abscissa) versus viscous modulus (ordinate) of skinned IFM fibers from *TmII* and *TmI/TmII* mutant lines. Data is plotted the same way as in Fig. 6. Again, note the progressive reduction in both viscous and elastic moduli and active loop size as the combined *TmI* and *TmII* gene copy number decreases from three (P[TmI^{+}];*Df(3R)* ea^{5022}/*TM3*) to two (*Df[3R]* ea^{5022}/*TM3*) to essentially one (*Df[3R]*ea^{5022}/*Ifm(3)3*). Note the X axes vary in the figure parts.

and 34 have tropomyosin domains similar to Ifm-TmI suggest that all three tropomyosin isoforms may co-assemble onto thin filaments in wild-type IFM. Therefore, it may be possible for TnH-33 and 34 to occupy some of the Ifm-TmI binding sites which are vacant in the transheterozygous IFM. Supporting this view, TnH-33 and 34 protein levels in the IFM are normal in an *Ifm(3)3/Ifm(3)3* mutant background (Mogami and Hotta, 1981), indicating that a reduction in Ifm-TmI does not affect the accumulation of TnH-33 and -34. Further, it has been shown that end-to-end interactions between tropomyosin molecules (something which may not be possible between adjacent TnH molecules because of their hydrophobic COOH-terminal domains), is not required for the stabilization of thin filaments during assembly (Butters et al., 1993). Therefore, it is possible that the TnH isoforms may substitute for or combine with residual Ifm-TmI in the transheterozygotes to form small but organized fibrillar cores.

The structural pertubations in the IFM caused by reducing the TnH isoforms by half were not as severe as the disordered filament lattice caused by reducing Ifm-TmI by half. A *TmII* heterozygote had neatly assembled fibrils which were ~80% the size of wild type fibrils, whereas a *TmI* heterozygote had disrupted myofibrils which were ~50% that of wild type. These differences in myofibrillar structure in fibers with reduced levels of either Ifm-TmI or TnH-33 and -34 may reflect the different structural roles of the *TmI* and *TmII* encoded tropomyosin isoforms which may, in turn, reflect different protein stoichiometries of Ifm-TmI vs. TnH-33 and -34 in the IFM. It is possible that the molar ratio of the TnH isoforms is low compared to Ifm-TmI and that myofibers can tolerate an ~50% reduction in TnH, but not Ifm-TmI, with no severe structural effects. Our results show the TnH isoforms do contribute to the complete lattice structure of myofibrils because reduction of TnH by mutation reduced the size of the ordered fibrillar cores. These data indicate that TnH-33 and -34 are structural proteins required for normal fibrillar assembly in the IFM, although compared with Ifm-TmI, their structural role(s) appear to be minor.

The similarity in the ultrastructural disruptions observed between the null TmI^{C10} and the *TmI* nonsense mutants, TmI^{J8} and TmI^{L2}, suggests that the nonsense mutants may be null mutants as well, possibly because they produce truncated or unstable Ifm-TmI proteins which cannot assemble onto thin filaments. It was surprising, however, that the missense mutant TmI^{S2}, which caused a charge change, also resulted in a null-like phenotype. One explanation is that the single amino acid change produces an unstable Ifm-TmI protein which is then degraded. A second possibility, however, is that the negative charge at Asp121, absent in the TmI^{S2} mutant, is important for the function and/or structure of muscle tropomyosins. An Asp at residue 121 is conserved through evolution, including tropomyosins of human skeletal muscle (α isoform), rabbit skeletal muscle, chicken skeletal and smooth muscle,

equine platelet, and all muscle isoforms of the *Drosophila TmI* and *TmII* genes (see Basi and Storti, 1986; Hanke and Storti, 1988). Interestingly, a Asp175>Asn mutation (D175N) at another conserved, charged residue in human skeletal α-tropomyosin causes familial hypertrophic cardiomyopathy (Thierfelder et al., 1994). Recently, An et al. (1996. *Biophys. J.* 70:A39) reported that human D175N α-tropomyosin has a twofold weaker affinity for actin in vitro than does human wild-type α-tropomyosin, suggesting that the D175N mutation affects tropomyosin's ability to bind actin in vivo. The conservation of charged residues in tropomyosin may be critical for intra- or intermolecular protein/protein interactions depending on the location of the residue in the α-helix. According to the heptapeptide repeat unit described by McLachlan and Stewart (1975), Asp121 of *Drosophila TmI*, like the D175N residue in human α-tropomyosin, lies on the outer surface of the Tm helix and may be involved in binding tropomyosin to another myofibrillar protein such as actin.

Mechanics of Tm⁻ Fibers

The mechanical parameters of the *Tm* mutant skinned fibers including isometric tension, dynamic stiffness, and power production, indicated a decrease in muscle performance as the organized fibrillar cores were reduced in diameter by the loss of Ifm-TmI and/or TnH-33 and 34. In our previous analysis of the *TmI* hypomorph *Ifm(3)3*, we observed that dynamic stiffness of the Ca^{2+}-activated IFM was reduced in proportion to the filament lattice disruption, resulting in a concomitant drop in wing beat frequency (Molloy et al., 1992). Since the resonant frequency of the flight muscle is proportional to the square root of the stiffness of the wing mount (cuticle and muscles) (Pringle, 1957), the results implied that most of the mounting stiffness was in the flight muscle. The results described here, comparing wing beat frequency, lattice disruption and dynamic stiffness of Ifm-TmI and TnH-33 and -34 mutant fibers are consistent with this view. That is, the decrease in dynamic stiffness of the mutant fibers paralleled the decrease in the diameter of the organized fibrillar cores, and the square root of the dynamic stiffness dropped proportionately with the wing beat frequency.

Ifm-TmI Tropomyosin Deficiency Caused Relaxed Fiber Responses

The relaxed responses from the transheterozygous fibers severely deficient in Ifm-TmI tropomyosin suggested that some myofibrillar defect caused by the reduction of sarcomeric tropomyosin restricts, inhibits or abolishes the formation of strong, force-generating cross-bridges. These results were similar to the results obtained for *Ifm(3)3/Ifm(3)3* fibers (Molloy et al., 1992). In both studies, fibers that were severely deficient in Ifm-TmI tropomyosin did not generate significant isometric force in activating conditions, nor were they able to produce any appreciable power despite organized fibrillar cores measuring ~20% that of wildtype (electron micrographs of skinned fibers showed that fibrillar cores of the transheterozygotes remained intact after detergent treatment; data not shown). The approximate fourfold increase in dynamic stiffness of the transheterozygous fibers after ATP depletion (i.e., rigor) indicated that actomyosin cross-bridges can form in these mutant muscles and argues that thick and thin filaments in the organized core of the mutant fibrils are spatially oriented to allow cross-bridge interactions to occur. We consider four possible explanations which singly or in combination may account for the relaxed dynamic responses of the mutant fibers.

(*a*) Hill et al. (1980) suggested that two forms of actin, inactive and active, exist in equilibrium with each other until the rise of Ca^{2+} and the cooperative binding of strong myosin cross-bridges shifts the equilibrium in favor of the active state of actin. Weak myosin cross-bridges bound to "inactive" actin must be formed first and are a prerequisite for the formation of strong myosin cross-bridges (Chalovich et al., 1991). According to the allosteric model (reviewed in Chalovich, 1993) Ifm-TmI associated with the thin filament may be needed to position actin in an "active" conformational state for the formation of active, force-generating cross-bridges. Thus, the relaxed responses we observed in fibers deficient in Ifm-TmI may result from some actin remaining in an inactive state even in the presence of Ca^{2+}.

(*b*) Direct measurement of actin stiffness in isolated thin filaments (Kojima et al., 1993) indicated thin filament compliance is nearly twofold greater in the absence of tropomyosin than in its presence. The comparatively high compliance of Ifm-TmI deficient thin filaments may be due to loss of actin rigidity, and thus, the ability to transmit active force during length perturbations may be compromised in the transheterozygous fibers.

(*c*) Granzier and Wang (1993) proposed a passive stretch sensor, the connecting filament (likely to be projectin, i.e., *Drosophila* titin) links the Z bands to the thick filaments. Upon muscle stretch, projectin transmits a strain to the thick filament which promotes the formation of strong myosin crossbridges. The shortened sarcomeres and the tandem array of Z bands in the transheterozygous fibers suggest the continuity along the length of the myofibrils is perturbed and this may impact on the function of projectin. Therefore, the relaxed response of the transheterozygous fibers might be partially the result of disrupted connecting filaments which are unable to transmit sufficient strain to the thick filaments to induce strong myosin cross-bridge formation.

(*d*) There may be redundancies in the function of the tropomyosin isoforms, such that TnH-33 and -34 substitute for the standard tropomyosin in the mutants, as these isoforms may also bind actin through their tropomyosin domain. In this scenario, the proline-rich COOH-terminal domain of TnH which lies adjacent to the rear cross-bridge in *Lethocerus* thin filaments may sterically block or interfere with actomyosin interactions (Reedy et al., 1994*a*); alternatively, it is also possible that the tropomyosin domain of TnH may block the binding site on actin for strong, force generating crossbridges. The expectation from this idea is that reducing TnH isoforms in a fiber severely depleted for Ifm-TmI should increase the dynamic stiffness. We did see a trend in this direction but the change was not significant (Table II, 79 ± 30 N m^{-2} with TnH [TmI^{C10}/*Ifm(3)3*] vs. 92 ± 18 N m^{-2} with reduced TnH [*Df(3R)* ea^{5022}/*Ifm(3)3*)]. An expanded study measuring the dynamic stiffness of more fibers may confirm this trend.

Stretch Activation of the IFM Is Not Affected in a TnH Heterozygote

The overall effect on flight ability and flight muscle structure and power output caused by reducing the TnH isoforms by ~50% was unexpectedly mild, particularly when compared with the structure and power output of fibers with ~50% Ifm-TmI. As noted above, reducing the levels of TnH-33 and -34 tropomyosin (as in P[TmI^+]$Df(3R)ea^{5022}$/+, Fig. 4, *c* and *d*) only reduced the diameter of myofibrils but did not cause the substantial filament splaying and accompanying structural disruptions observed in the *TmI* heterozygote (TmI^{C10}/+, Fig. 4, *e* and *f*). There was no difference in maximal isometric tension in the *TmI vs. TmII* deficient fibers (0.84 ± 0.7 kN/m^2 for TmI^{C10}/+ vs. 0.90 ± 0.6 kN/m^2 for P[TmI^+]$Df(3R)ea^{5022}$/+); however, the force levels in all *Tm* mutants analyzed here are very low and differences would be difficult to resolve. In contrast, differences in maximal power output were reasonably well resolved in the mutants and our results showed *TmII* mutants were much less affected than *TmI* mutants (73% of wild type in *TmII* heterozygote vs. 32% of wild type in *TmI* heterozygote, see Table II). The 27% power reduction in the *TmII* mutants was not severe enough to prevent flight (Table II). These results show the IFM can tolerate a significant reduction in TnH with little effect on function.

This finding does not appear to support the postulated role of TnH in the so called "stretch sensor" which may form a link between the thick and thin filaments and be important for the response to stretch (Reedy et al., 1994*a*; Tohtong et al., 1995). One would have predicted a more dramatic effect in a fiber with a 50% reduction in a stretch sensor component. However, it will be necessary to analyze IFM which completely lacks the TnH isoforms to critically test the role of TnH in stretch activation. The mild effect on power output we observed in the *TmII* heterozygote may be a consequence of the involvement of multiple proteins in the response to stretch. This seems likely since TnH is also found in muscle which is not stretch activated (Peckham et al., 1992). Likely candidates for additional stretch sensor components include the IFM-specific isoforms of troponin subunit I (Barbas et al., 1991; Beall and Fyrberg, 1991) and arthrin (ubiquitinated actin) (Ball et al., 1987). Another interesting possibility is that a link between the *Drosophila* myosin regulatory light chain (MLC-2) and actin or arthrin exists as suggested by recent NMR studies (Trayer, I., J. Moore, D. Timson, and D.W. Maughan, unpublished results).

Activation of muscle contraction in insect flight muscle is a coordinated series of events that relies not only on the Ca^{2+}-sensitive interaction of myosin and actin, but also on the coordinated response of a number of proteins to mechanical stretch. In a recent review of tropomyosin function, Reedy et al. (1994*b*) suggested that tropomyosin's role in thin filament regulation may be expanded to that of both a steric blocking protein and an allosteric effector of actin conformation change. One possibility for the IFM is that this dual role is divided between the two types of tropomyosin, such that Ifm-TmI effects a conformational change in actin and the TnH isoforms sterically block actomyosin interactions.

We remember the inspiration and dedication of our late colleague and friend Dr. Scott Falkenthal. We thank Dr. J. Warmke for his help in isolating the TmI mutants, Drs. J. Molloy and J. Sparrow for their excellent counsel and suggestions on the mechanics of the IFM, Dr. J. Clayton for his helpful advice on IFM protein isolation, Dr. C. Beall for critically reading the manuscript, Dr. E.A. Fyrberg for the 88F clones, Dr. R. Storti for fly stocks, and Dr. K.V. Anderson for fly stocks and suggestions on the embryo squash technique. We also acknowledge the technical help of J. Hurley, G. Sleeper, and B. Barnes.

This work is supported by National Institutes of Health grant AR40234-03.

Received for publication 27 March 1996 and in revised form 13 August 1996.

References

Adelstein, R.S., and E. Eisenberg. 1980. Regulation and kinetics of the actin-myosin-ATP interaction. *Ann. Rev. Biochem.* 49:921–956.

Ball, E., C. Karlik, C. Beall, D. Saville, J. Sparrow, B. Bullard, and E. Fyrberg. 1987. Arthrin, a myofibrillar protein of insect flight muscle, is an actin-ubiquitin conjugate. *Cell.* 51:221–228.

Barbas, J.A., J. Galceran, I. Krah-Jentgens, J.L.d.l. Pompa, I. Canal, O. Pongs, and A. Ferrus. 1991. Troponin I is encoded in the haplolethal region of the Shaker gene complex of Drosophila. *Genes Dev.* 5:132–140.

Basi, G.S., M. Boardman, and R.V. Storti. 1984. Alternative splicing of a Drosophila tropomyosin gene generates muscle tropomyosin isoforms with different carboxy-terminal ends. *Mol. Cell. Biol.* 4:2828–2836.

Basi, G.S., and R.V. Storti. 1986. Structure and DNA sequence of the Tropomysoin I gene from *Drosophila melanogaster*. *J. Biol. Chem.* 261:817–827.

Beall, C.J., and E. Fyrberg. 1991. Muscle abnormalities in *Drosophila melanogaster* heldup mutants are caused by missing or aberrant troponin I isoforms. *J. Cell Biol.* 114:941–951.

Bernstein, S.I., P.T. ODonnell,'and R.M. Cripps. 1993. Molecular genetic analysis of muscle development, structure, and function of Drosophila. *Int Rev. Cytol.* 143:63–152.

Broschat, K.O. 1990. Tropomyosin prevents depolymerization of actin filaments from the pointed end. *J. Biol. Chem.* 265:21323–21329.

Bullard, B., K. Leonard, A. Larkins, G. Butcher, C. Karlik, and E. Fyrberg. 1988. Troponin of asynchronous flight muscle. *J. Mol. Biol.* 204:621–637.

Butters, C.A., K.A. Willadsen, and L.S. Tobacman. 1993. Cooperative interactions between adjacent troponin–tropomyosin complexes may be transmitted through the actin filament. *J. Biol. Chem.* 268:15565–15570.

Chalovich, J.M. 1993. Actin mediated regulation of muscle contraction. *Pharmac. Ther.* 55:95–148.

Chalovich, J.M., L.C. Yu, and B. Brenner. 1991. Involvment of weak binding crossbridges in force production in muscle. *J. Mus. Res. Cell. Motil.* 12:503–506.

Craymer, L. 1984. Report. Drosophila Information Service. 60:234–236.

Cripps, R.M., and J.C. Sparrow. 1992. Polymorphism in a Drosophila indirect flight muscle-specific tropomyosin isozyme does not affect flight ability. *Biochemical Genetics.* 30:159–168.

El-Saleh, S.C., K.D. Warber, and J.D. Potter. 1986. The role of tropomyosin-troponin in the regulation of skeletal muscle contraction. *J. Mus. Res. Cell. Motil.* 7:387–404.

Erdelyi, M., and J. Szabad. 1989. Isolation and characterization of dominant female sterile mutations of *Drosophila melanogaster*. I. Mutations on the third chromosome. *Genetics.* 122:111–127.

Erdelyi, M., A.M. Michon, A. Guichet, J.B. Glotzer, and A. Eprussi. 1995. Requirement for Drosophila cytoplasmic tropomyosin in oskar mRNA localization. *Nature (Lond.).* 377:524–527.

Falkenthal, S., V.P. Parker, W.W. Mattox, and N. Davidson. 1984. *Drosophila melanogaster* has only one myosin alkali light-chain gene which encodes a protein with considerable amino acid sequence homology to chicken myosin alkali light chains. *Mol. Cell. Biol.* 4:956–965.

Fyrberg, E., and C. Beall. 1990. Genetic approaches to myofibril form and function in Drosophila. *Trends Genet.* 6:126–131.

Fyrberg, E., C. Fyrberg, C. Beall, and D.L. Saville. 1990. *Drosophila melanogaster* troponin T mutations engender three distinct syndromes of myofibrillar assembly. *J. Mol. Biol.* 216:657–675.

Granzier, H.L.M., and K. Wang. 1993. Interplay between passive tension and strong and weak binding cross-bridges in insect flight muscle: a functional dissection by gelsolin-mediated thin filament removal. *J. Gen. Physiol.* 101: 235–270.

Gremke, L., P.C. Lord, L. Sabacan, S.C. Lin, A. Wohlwill, and R.V. Storti. 1993. Coordinate regulation of Drosophila tropomyosin gene expression is controlled by multiple muscle-type-specific positive and negative enhancer elements. *Dev. Biol.* 159:513–527.

Hanke, P.D., and R.V. Storti. 1988. *The Drosophila melanogaster* tropomyosin II gene produces multiple proteins by use of alternative tissue-specific promoters and alternative splicing. *Mol. Cell. Biol.* 8:3591–3602.

Haselgrove, J.C., and H.E. Huxley. 1973. X-ray evidence for radial cross-bridge movement and for the sliding filament model in actively contracting skeletal

muscle. *J. Mol. Biol.* 77:549–568.
Hill, T.L., E. Eisenberg, and L.E. Greene. 1980. Theoretical model for the cooperative equilibrium binding of myosin subfragment 1 to the actin-troponin-tropomyosin complex. *Proc. Natl. Acad. Sci. USA.* 77:3186–3190.
Hitchcock-DeGregori, S.E., P. Sampath, and T.D. Pollard. 1988. Tropomyosin inhibits the rate of actin polymerization by stabilizing actin filaments. *Biochemistry.* 27:9182–9185.
Hyatt, C.J., and D.W. Maughan. 1994. Fourier analysis of wing beat signals: assessing the effects of genetic alterations of flight muscle structure in Diptera. *Biophys. J.* 67:1149–1154.
Karlik, C.C., and E.A. Fyrberg. 1985. An insertion within a variably spliced Drosophila tropomyosin gene blocks accumulation of only one encoded isoform. *Cell.* 41:57–66.
Karlik, C.C., and E.A. Fyrberg. 1986. Two *Drosophila melanogaster* tropomyosin genes: structural and functional aspects. *Mol. Cell. Biol.* 6:1965–1973.
Karlik, C.C., J.W. Mahaffey, M.D. Coutu, and E.A. Fyrberg. 1984. Organization of contractile protein genes within the 88F subdivision of the *D. melanogaster* third chromosome. *Cell.* 37:469–481.
Kawai, M., and P.W. Brandt. 1980. Sinusoidal analysis: a high resolution method for correlating biochemical reactions with physiological processes in activated skeletal muscles of rabbit, frog and crayfish. *J. Muscle Res. Cell. Motil.* 1:279–303.
Kojima, H., A. Ishijima, and T. Yanagida. 1994. Direct measurement of stiffness of single actin filaments with and without tropomyosin by in vitro nanomanipulation. *Proc. Natl. Acad. Sci. USA.* 91:12962–12966.
Lehman, W., R. Craig, and P. Vibert. 1994. Ca^{2+}-induced tropomyosin movement in Limulus thin filaments revealed by three-dimensional reconstruction. *Nature (Lond.).* 368:65–67.
Lehrer, S.S. 1994. The regulatory switch of the muscle thin filament: Ca^{2+} or myosin heads? *J. Muscle Res. Cell. Motil.* 15:232–236.
Lindsley, D.L., and G.G. Zimm. 1992. The Genome of *Drosophila melanogaster.* Academic Press, Inc., San Diego, CA. 1133 pp.
Liu, H., and A. Bretscher. 1989. Disruption of the single tropomyosin gene in yeast results in the disappearance of actin cables from the cytoskeleton. *Cell.* 57:233–242.
Maughan, D.W., and R.E. Godt. 1989. Equilibrium distribution of ions in a muscle fiber. *Biophys. J.* 56:717–722.
McLachlan, A.D., and M. Stewart. 1975. Tropomyosin coiled-coil interactions: evidence for an unstaggered structure. *J. Mol. Biol.* 98:293–304.
Miller, R.C., R. Schaaf, D.W. Maughan, and T.R. Tansey. 1993. A non-flight muscle isoform of Drosophila tropomyosin rescues an indirect flight muscle tropomyosin mutant. *J. Muscle Res. Cell. Motil.* 14:85–98.
Mogami, K., and Y. Hotta. 1981. Isolation of Drosophila flightless mutants which affect myofibrillar proteins of indirect flight muscle. *Mol. Gen. Genet.* 183:409–417.
Mogami, K., S.C. Fujita, and Y. Hotta. 1982. Identification of Drosophila indirect flight muscle myofibrillar proteins by means of two-dimensional electrophoresis. *J. Biochem. (Tokyo).* 91:643–650.
Molloy, J., A. Kreuz, R. Miller, T. Tansey, and D. Maughan. 1992. Effects of tropomyosin deficiency in flight muscle of *Drosophila melanogaster. In* Mechanism of Myofilament Sliding in Muscle. H. Sugi and G. Pollack, editors. Plenum Press, New York. pp. 165–172.
Mullis, K.B. 1991. The polymerase chain reaction in an anemic mode: how to avoid cold oligodeoxyribonuclear fusion. *PCR Meth. Appl.* 1:1–4.
Mullins, J.I., J. Casey, M.O. Nicholson, K.B. Burck, and N. Davidson. 1981. Sequence arrangement and biological activity of cloned feline leukemia virus provirus from a virus-productive human cell line. *J. Virol.* 38:688–703.
Peckham, M., J.E. Molloy, J.C. Sparrow, and D.C.S. White. 1990. Physiological properties of the dorsal longitudinal flight muscle and the tergal depressor of the trochanter muscle of *Drosophila melanogaster. J. Muscle Res. Cell. Motil.* 11:203–215.
Peckham, M., R. Cripps, D. White, and B. Bullard. 1992. Mechanics and protein content of insect flight muscles. *J. Exp. Biol.* 168:57–76.
Pringle, J.W.S. 1957. Insect Flight. Cambridge University Press, Cambridge. pp. 133.
Pringle, J.W.S. 1978. The Croonian Lecture. 1977. Stretch activation of muscle: function and mechanism. *Proc. R. Soc. London B.* 201:107–130.
Reedy, M.C., and C. Beall. 1993. Ultrstructure of developing flight muscle in Drosophila. I. Assembly of myofibrils. *Dev. Biol.* 160:443–465.
Reedy, M.C., C. Beall, and E. Fyrberg. 1989. Formation of reverse rigor chevrons by myosin heads. *Nature (Lond.).* 339:481–483.
Reedy, M.C., M.K. Reedy, K.R. Leonard, and B. Bullard. 1994*a*. Gold/Fab immuno electron microscopy localization of troponin H and troponin T in Lethocerus flight muscle. *J. Mol. Biol.* 239:52–67.
Reedy, M.K., M.C. Reedy, and F. Schachat. 1994*b*. Tropomyosin: does resolution lead to reconciliation? *Curr. Biol.* 4:624–626.
Saiki, R.K., D.H. Gelfand, S. Stoeffel, S.J. Scharf, R. Higuchi, G.T. Horn, K.B. Mullis, and H.A. Erlich. 1988. Primer-directed enzymatic amplification of DNA with a thermostable DNA polymerase. *Science (Wash. DC).* 239:487–491.
Sanger, F., S. Nicklen, and A.R. Coulson. 1977. DNA sequencing with chain-terminating inhibitors. *Proc. Natl. Acad. Sci. USA.* 74:5463–5467.
Schultz, J.R., T. Tansey, L. Gremke, and R.V. Storti. 1991. A muscle-specific enhancer required for rescue of indirect flight muscle and jump muscle function regulates Drosophila tropomyosin I gene expression. *Mol. Cell. Biol.* 11: 1901–1911.
Shafiq, A. 1963. Electron microscopic studies on the indirect flight muscles of *Drosophila melanogaster.* I. Structure of the myofibrils. *J. Cell Biol.* 17:351–362.
Southern, E.M. 1975. Detection of specific sequences among DNA fragments separated by gel electrophoresis. *J. Mol. Biol.* 98:503–517.
Sparrow, J., M. Reedy, E. Ball, V. Kyrtatas, J. Molloy, J. Durston, E. Hennessey, and D. White. 1991*a*. Functional and ultrastructural effects of a missense mutation in the indirect flight muscle-specific actin gene of Drosophila melanogaster. *J. Mol. Biol.* 222:963–982.
Sparrow, J., D. Drummond, M. Peckham, E. Hennessey, and D. White. 1991*b*. Protein engineering and the study of muscle contraction in Drosophila flight muscles. *J. Cell. Sci.* 14 (Suppl.):73–78.
Squire, J.M. 1994. The actomyosin interaction-shedding light on structural events: "plus ca change, plus c'est la meme chose." *J. Muscle Res. Cell Motil.* 15:227–231.
Steiger, G.J. 1977. Tension transients in extracted rabbit heart muscle preparations. *J. Mol. Cell. Cardiol.* 9:671–685.
Tansey, T., M.D. Mikus, M. Dumoulin, and R.V. Storti. 1987. Transformation and rescue of a flightless Drosophila tropomyosin mutant. *EMBO (Eur. Mol. Biol. Organ.) J.* 6:1375–1385.
Tawada, K., and M. Kawai. 1990. Covalent crosslinking of single fibers from rabbit psoas increases oscillatory power. *Biophys. J.* 57:643–647.
Thierfelder, L., H. Watkins, C. MacRae, R. Lamas, W. McKenna, H.-P. Vosberg, J.G. Seidman, and C.E. Seidman. 1994. α-tropomyosin and cardiac troponin T mutations cause familial hypertrophic cardiomyopathy: a disease of the sarcomere. *Cell.* 77:701–712.
Thorson, J., and D.C.S. White. 1983. Role of cross-bridge distortion in the small signal mechanical dynamics if insect and rabbit striated muscle. *J. Physiol.* 343:59–84.
Tohtong, R., H. Yamashita, M. Graham, J. Haeberle, A. Simcox, and D. Maughan. 1995. Impairment of muscle function caused by mutations of phosphorylation sites in myosin regulatory light chain. *Nature (Lond.).* 374: 650–653.
Warmke, J.W., A.J. Kreuz, and S. Falkenthal. 1989. Co-localization to chromosome bands 99E1-3 of the *Drosophila melanogaster* myosin light-chain 2 gene and a haplo-insufficient locus that affects flight behavior. *Genetics.* 122: 139–151.
Warmke, J., M. Yamakawa, J. Molloy, S. Falkenthal, and D. Maughan. 1992. Myosin light chain-2 mutation affects flight, wing beat frequency, amd indirect flight muscle contraction kinetics in Drosophila. *J. Cell. Biol.* 119:1523–1539.
Weigt, C., B. Schoepper, and A. Wegner. 1990. Tropomyosin–troponin complex stabilizes the pointed ends of actin filaments against polymerization and depolymerization. *FEBS Lett.* 260:266–268.
Zhao, Y., and M. Kawai. 1993. The effect of the lattice spacing change on cross-bridge kinetics in chemically skinned rabbit psoas muscle fibers. II. Elementary steps affected by the spacing change. *Biophys. J.* 64:197–210.